Layer analysis of the structure of water confined in vycor glass

P. Gallo, M. A. Ricci, and M. Rovere[a]

Dipartimento di Fisica "E. Amaldi," Università degli Studi "Roma Tre," Istituto Nazionale per la Fisica della Materia, Unità di Ricerca Roma Tre Via della Vasca Navale 84, 00146 Roma, Italy

A molecular dynamics simulation of the microscopic structure of water confined in a silica pore is presented. A single cavity in the silica glass has been modeled as to reproduce the main features of the pores of real Vycor glass. A layer analysis of the site–site radial distribution functions evidences the presence in the pore of two subsets of water molecules with different microscopic structure. Molecules which reside in the inner layer, close to the center of the pore, have the same structure as bulk water but at a temperature of 30 K higher. On the contrary the structure of the water molecules in the outer layer, close to the substrate, is strongly influenced by the water–substrate hydrophilic interaction and sensible distortions of the H-bond network and of the orientational correlations between neighboring molecules show up. Lowering the hydration has little effect on the structure of water in the outer layer. The consequences on experimental determinations of the structural properties of water in confinement are discussed. © *2002 American Institute of Physics.* [DOI: 10.1063/1.1423662]

I. INTRODUCTION

The observation that in many real situations water is confined (in a rock, in a cell, in a microemulsion, in an ionic channel, in interstellar bodies, etc.) explains the large interest devoted to structural and dynamical properties of water in restricted geometries. During the last decade indeed several experiments have been performed by using different techniques and different confining substrates, that have evidenced a rich variety of phenomena, sometimes even more puzzling than those known for bulk water.[1] Moreover recent theoretical studies have evidenced for confined water a thermodynamics more complex than that of bulk water.[2]

In particular the comparison of the properties of bulk and confined water that emerges from different experiments is sometimes misleading. As a matter of fact the slowing down of the translational and rotational motion upon confinement, evidenced by nuclear magnetic resonance (NMR) (Ref. 3) and quasielastic neutron scattering (QENS),[4] apparently contrasts with the lower average density deduced for confined water with respect to the bulk state by small angle neutron scattering (SANS).[5] Moreover neutron diffraction (ND) experiments on pure D_2O have been interpreted in terms of an increased number of hydrogen bonds (HB) upon confinement;[6] while experiments exploiting the isotopic H/D substitution on water reveal a reduction of such bonds and a lower tetrahedral order,[7,8] in agreement with x-ray diffraction.[6] On the other hand the analysis of the temperature derivatives of the radial distribution functions (RDF) of confined and bulk D_2O suggests that the structural rearrangement upon lowering the temperature is the same for the two systems.[9] More recently the idea has been put forward that lowering the amount of water inside the confining matrix is

equivalent to lowering the temperature in bulk water.[6,10,11] Finally, besides and in partial disagreement with these interpretations of the experimental findings, two experimental evidences are well established:

(1) confined water can be easily supercooled down to lower temperatures compared to the bulk;
(2) the lower the hydration level, the lower the ice nucleation temperature.

The observation that the density profile of water in restricted geometries is not uniform,[12–17] whatever the substrate–water interaction is, suggests that most of the misfits between the experimental observations reported above are due to averaging the response of different water layers, that cannot be easily isolated in the experiments, unless an accurate study as a function of the hydration level is performed. Molecular dynamics (MD) simulations performed in realistic environments can be then of great help in better interpreting the experimental data. As a matter of fact the system that has been more widely used by the experimentalists[4,5,7,8,10,11,18–20] to confine water, namely, porous Vycor glass,[21] has also the advantage of being a simple molecular system, that can be computer simulated.[16,22] In the attempt of giving an harmonic interpretation of at least the structural properties of water in restricted geometries, we have performed a layer analysis of the microscopic structure of water in Vycor glass, at different temperatures and hydrations.

In Sec. II we briefly describe the simulation method. In Sec. III we discuss how the calculation of the pair correlation functions can be performed by taking into account the finite volume effects. In Sec. IV we introduce the layer analysis and present the main results. The last section is devoted to the conclusions.

[a] Author to whom correspondence should be addressed. Electronic mail: rovere@fis.uniroma3.it
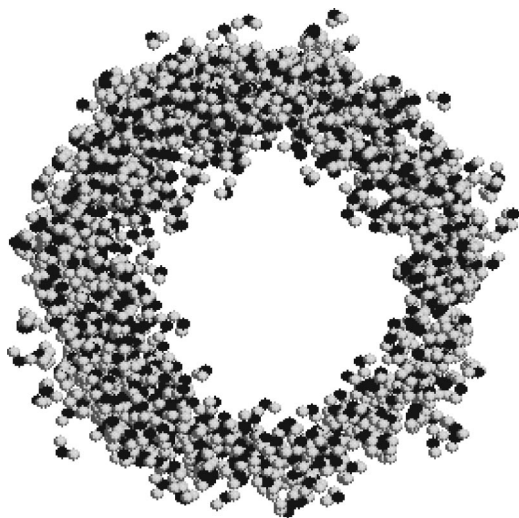
342

FIG. 1. Projection on the $x-y$ plane of a snapshot from simulation of 1500 molecules of pure SPC/E water inside a cylindrical cavity of Vycor glass. The radius of the cavity is 20 Å. For the sake of clarity only water molecules are shown. Oxygens are black and hydrogens are gray.

II. MOLECULAR DYNAMICS OF CONFINED WATER

The behavior of water confined in the pores of Vycor glass is influenced by both the geometrical effects and the interaction with the hydrophilic surfaces. In order to account for these effects in computer simulation we constructed a single pore of silica which reproduces the most relevant average features of the pores of real Vycor glass. As described in more detail in a previous work,[16] we carved a cylindrical pore of 40 Å diam in a cubic cell of silica glass obtained by the usual procedure of MD simulation. Then we prepared the cavity surface by removing the silicon atoms bonded to less than four oxygens. The oxygen atoms bonded to only one silicon (*nonbridging oxygens*) were saturated with acidic hydrogens. We note that since the surface of the cavity is rough its actual volume V_p is unknown and only roughly approximated to a lower value by the volume V_c of a cylinder of radius $R_c = 20$ Å.

Inside the pore a fixed number N_W of water molecules is inserted and the MD simulation is performed at constant density $\rho = N_W / V_c$ in the NVE ensemble. We assume, according to the experiments,[5,7] that at full hydration the density is $\rho_f = 0.0297$ Å^{-3}, corresponding to $N_W = 2600$. In the following we will present results for $N_W = 2600$ and $N_W = 1500$ which is roughly the half-hydration case.

Water–water and water–substrate interactions are respectively described by the SPC/E site model[23] and by an empirical potential model, consisting of Lennard-Jones and Coulomb forces. The potential parameters are those used and tabulated in Ref. 16, where further technical details can be found. During the MD runs the atoms of the Vycor glass are kept fixed. Periodic boundary conditions are applied along the axis of the cylinder (z-direction). The motion is confined in the $x-y$ plane.

A snapshot from the simulation of 1500 water molecules is presented in Fig. 1. Only water molecules are displayed, and the hydrophilic nature of the Vycor surface is evident, since all water molecules are attracted toward the substrate.

III. EXCLUDED VOLUME EFFECTS ON THE PAIR CORRELATION FUNCTIONS

The calculation of the site–site radial distribution functions (SSRDF) in computer simulation is not straightforward when dealing with a confined system, since excluded volume effects must be carefully taken into account.[8,17,24,25]

From the MD simulation we can calculate in the usual way the average number $n^{(2)}_{\alpha\beta}(r)$ of sites of type β lying in a spherical shell $\Delta v(r)$ at distance r from a site of type α. Then normalizing to the average number of atoms of an ideal gas at the same density in the same spherical shell, one obtains[26]

$$\tilde{g}_{\alpha\beta}(r) = \frac{n^{(2)}_{\alpha\beta}(r)}{\dfrac{N_\beta}{V_p}\Delta v(r)}, \tag{1}$$

where N_β is the total number of β sites and V_p is the volume of the simulation cell.

At variance with a bulk liquid, if we consider a collection of noninteracting particles in a confining volume, where periodic boundary conditions are, for instance, only along the z-axis, as in our case, the *uniform* radial distribution function is not simply $g_u(r) = 1$. It indeed depends on the geometry of the confining system and generally will not be a constant. Hence the functions defined in Eq. (1) must be further normalized to the uniform profile $g_u(r)$. In our case this is given by[17]

$$g_u(r) = \frac{V_p}{(2\pi)^3}\int d^3Q\, P_{\text{cyl}}(Q). \tag{2}$$

$P_{\text{cyl}}(Q)$ is the form factor of the cylindrical simulation cell of height L and radius R_c,[27]

$$P_{\text{cyl}}(Q) = \int_0^1 d\mu \left[j_0\left(\frac{\mu QL}{2}\right) \right]^2 \left[\frac{2 j_1(QR_c\sqrt{1-\mu^2})}{QR_c\sqrt{1-\mu^2}} \right]^2, \tag{3}$$

where $j_n(x)$ are the Bessel's functions of order n.

The properly normalized SSRDF are then obtained as

$$g_{\alpha\beta}(r) = \frac{\tilde{g}_{\alpha\beta}(r)}{f_c \cdot g_u(r)}. \tag{4}$$

The correction factor f_c accounts for the roughness of the surface and the already discussed uncertainty in the volume determination. It is adjusted to give the corrected pair correlation functions oscillating around 1 at large r.

The corrected SSRDF for the full hydration case are shown in Fig. 2 and are compared to the corresponding functions of SPC/E water at ambient conditions. As discussed in a previous work[17] the modifications of the oxygen–oxygen (OO) and of the oxygen–hydrogen (OH) functions relative to bulk water are in good qualitative agreement with the experiments.[8] For instance the first minimum of the OO function becomes shallower and fills in and the H-bond peak becomes less intense upon confinement.
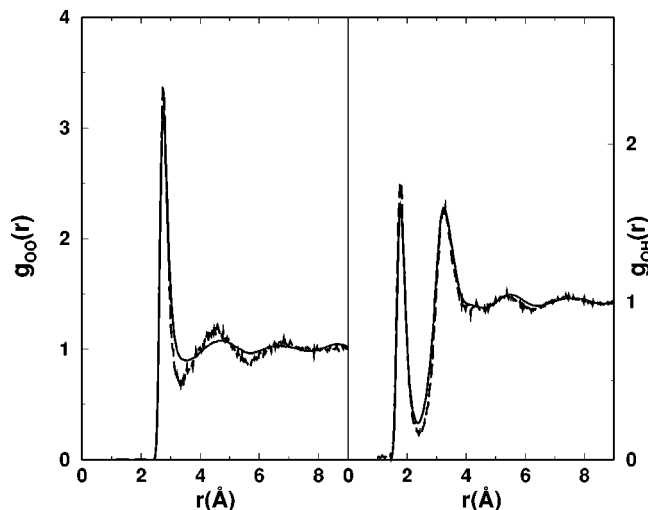
FIG. 2. Site–site radial distribution functions $g_{OO}(r)$ (on the left) and $g_{OH}(r)$ (on the right) at full hydration at $T = 298$ K (full line) compared with the same functions of the bulk water (long dashed line). The functions of the confined system have been calculated by using Eqs. (1)–(4).

IV. LAYERING EFFECT AND STRUCTURE OF CONFINED WATER

Looking at the density profile reported in the inset of Fig. 3 as a function of $R = \sqrt{x^2 + y^2}$ we see that the density profile is very flat in the range $0 < R < 15$ Å and its value is in agreement with the density of confined water at full hydration observed in the experiments. For $R > 15$ Å water adsorbs and a double layer structure is formed close to the surface. The double layer with density higher than the average extends for almost 3 Å. A depletion layer of 2 Å, due to the short range repulsion of the substrate is also visible.

We notice that the density profile is almost independent of the temperature.
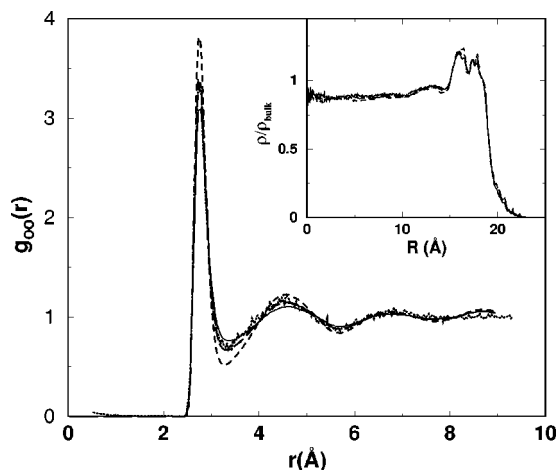

FIG. 3. Site–site radial distribution functions $g_{OO}(r)$ at full hydration calculated for the inner layer ($0 < R < 15$ Å, see text) at temperatures $T = 298$ K (continuous line), $T = 270$ K (long dashed line), and $T = 240$ K (short dashed) compared with the corresponding function of the bulk at ambient conditions (dotted line). The SSRDF of bulk water at ambient conditions is almost coincident with that of confined water at 270 K. In the inset the density profile at full hydration for $T = 298$ K, $T = 270$ K, and $T = 240$ K are reported by using the same symbols.

As a consequence of the hydrophilic interaction a strong distortion of the hydrogen bond network of water in the layers close to the substrate is observed.[16,17] Moreover this layering effect has important consequences on the dynamical behavior of water as recently shown.[28] It seems therefore appropriate to develop a layer analysis for the SSRDF by separating the contribution of the water molecules which spend most of the time in the internal layer ($0 < R < 15$ Å) from the contribution of the molecules belonging to the double layer or to the depletion layer.

A. Inner layer

The SSRDF in the inner layer can be obtained from the MD data by using Eqs. (1)–(4) where now the radius of the cylinder is $R_c = 15$ Å.

In Fig. 3 we show the resulting $g_{OO}(r)$ for the inner layer at different temperatures and compare with the equivalent function of ambient temperature SPC/E water.

We notice that the $g_{OO}(r)$ of the confined system are very similar to those of bulk water. In particular present data at $T = 270$ K superimpose to the oxygen–oxygen RDF calculated for bulk water at ambient conditions. For the other two SSRDF (not shown) we find the same result, suggesting that as far as the microscopic structure is concerned water confined in the middle of the pore behaves as bulk water at an higher temperature ($\Delta T \sim 30$ K). This result may explain why confined water can be more easily supercooled than the bulk.

B. Outer layer

In the calculation of the SSRDF for the outer layer the geometry of the confining volume and the form factor appearing in Eq. (2) are different from those used in the previous case. Now the function $g_u(r)$ must be calculated in the region $15 < R < 20$ Å, where the water is adsorbed on the surface. In doing so, we can assume that the uniform density of noninteracting atoms is different from zero and constant in the range $15 < R < 18$ Å, neglecting the small contribution which comes from particles in the depletion layer $18 < R < 20$ Å. The form factor to be used is now that of two concentric cylinders of radius $R_1 = 15$ Å and $R_2 = 18$ Å, respectively,

$$P_{diff}(Q) = \frac{1}{(V_2 - V_1)} [V_2 P_{cyl}^{(1)}(Q) - V_1 P_{cyl}^{(2)}(Q)], \qquad (5)$$

where V_i is the volume of the cylinder of radius R_i and $P_{cyl}^{(i)}(Q)$ is given by Eq. (3) with $R_c = R_i$.

In Fig. 4 we report the RDF of the oxygen sites obtained with this procedure together with the initial distribution $\tilde{g}_{OO}(r)$ calculated according to Eq. (1) and the uniform profile $g_u(r)$ for the concentric cylinders. We notice that the correction for the excluded volume effects may still be not completely satisfactory in the region of the main peak, due to neglecting the presence of the depletion layer. In spite of this we can infer that the structure of water in the double layer close to the substrate is strongly distorted with respect to the bulk. The $g_{OO}(r)$ function does not show any feature typical of the tetrahedral arrangement of H-bonded molecules. In
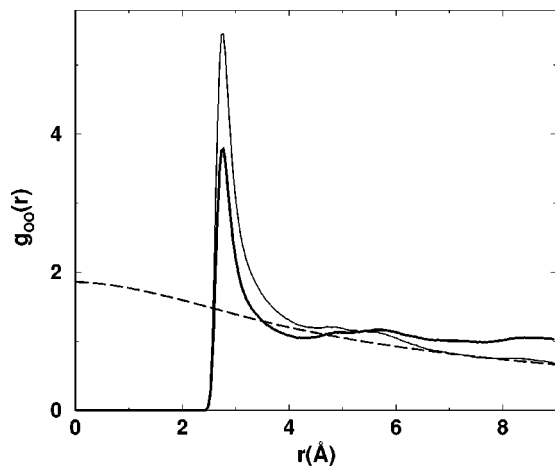
FIG. 4. Site–site radial distribution functions $g_{OO}(r)$ at full hydration cal-culated for the outer layer ($15<R<20$ Å) at temperatures $T=298$ K. Thin-ner solid line is $\tilde{g}_{OO}(r)$ defined in Eq. (1); dashed line is the uniform profile calculated according to Eq. (2). The corrected RDF is reported as a thick solid line.

FIG. 6. Site–site radial distribution functions $g_{OH}(r)$ (on the left) and $g_{HH}(r)$ (on the right) at full hydration calculated for the outer layer ($15<R<20$ Å) at temperatures $T=298$ K (full line), $T=270$ K (long dashed line), $T=240$ K (short dashed line).

particular the second peak is shifted to higher distances and its intensity is much reduced with respect to the bulk water case. We observe also that the $g_{OO}(r)$ of the outer layer does not change much with the temperature, as can be seen in Fig. 5; only a sharpening of the main peak at the lowest tempera-ture is visible.

The $g_{OH}(r)$ and $g_{HH}(r)$ functions calculated for the outer layer are reported in Fig. 6 at different temperatures. At variance with the $g_{OO}(r)$ these functions show the main peaks at about the same r-values as their analogous functions obtained for bulk water. Yet differences are observed in the relative intensity of the first two peaks; these may be par-tially ascribed to residual excluded volume effects due to the presence of the depletion layer. Also the $g_{OO}(r)$ and $g_{OH}(r)$ functions are weakly temperature dependent.
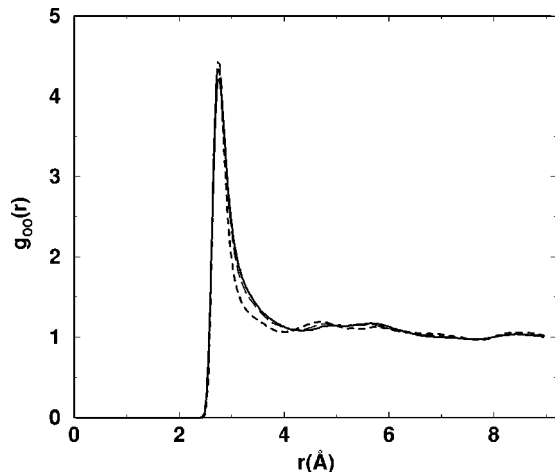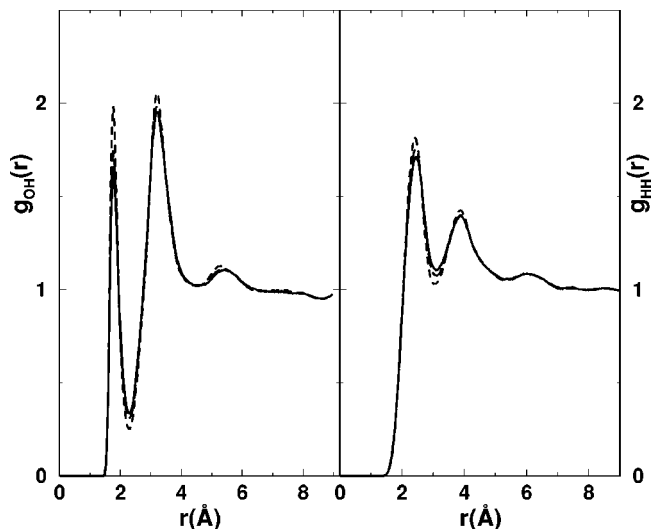
C. Half-hydration

The density profile calculated at half hydration (N_W = 1500) evidence the presence of a double layer of adsorbed water molecules, with the same characteristics as in the full hydration case. Thus we can calculate the SSRDF for the outer layer by using the uniform profile calculated in the previous section for the full hydration case [Eq. (5)].

In Fig. 7 we compare the $g_{OO}(r)$ functions at the two hydration levels investigated, at room temperature. In Fig. 8 the same comparison is done for the $g_{OH}(r)$ and $g_{HH}(r)$ functions. It is clear from these figures that changing the hydration does not affect the SSRDF of the outer layer; the same evidence is found at the other investigated tempera-tures.
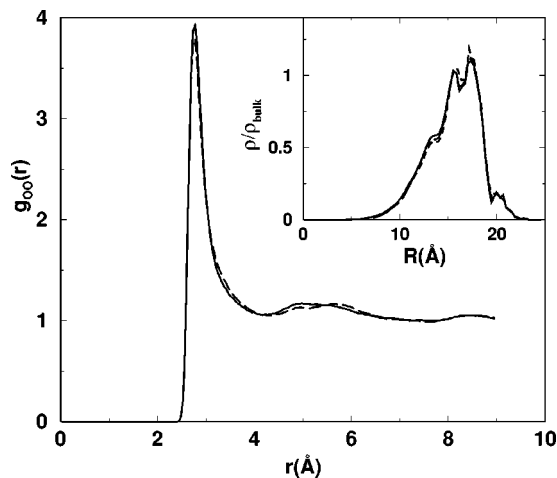

FIG. 5. Site–site radial distribution functions $g_{OO}(r)$ at full hydration cal-culated for the outer layer ($15<R<20$ Å) at temperatures $T=298$ K (full line), $T=270$ K (long dashed line), $T=240$ K (short dashed line).

FIG. 7. Site–site radial distribution functions $g_{OO}(r)$ calculated for the outer layer ($15<R<20$ Å) at half-hydration (full line) compared with the same function at full hydration (long dashed line) at temperatures $T=298$ K. In the inset the density profile at half hydration for $T=298$ K (full line), $T=270$ K (long dashed line), and $T=240$ K (short dashed line) are reported.
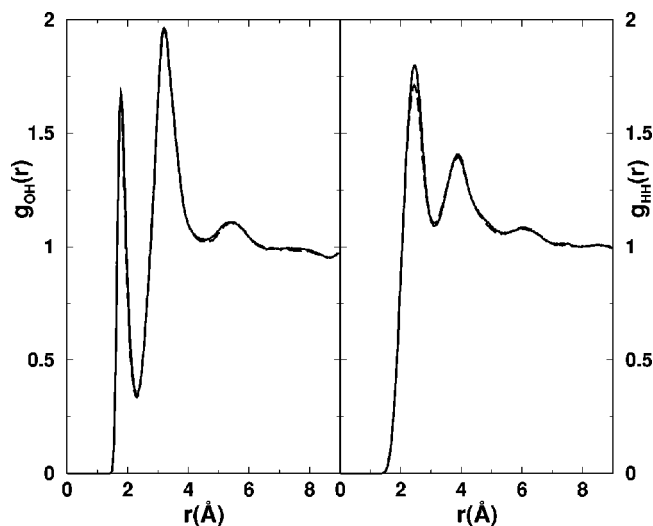
FIG. 8. Site–site radial distribution functions $g_{OH}(r)$ (on the left) and $g_{HH}(r)$ (on the right) at half hydration (full line) calculated for the outer layer ($15 < R < 20$ Å) compared with the same functions at full hydration (long dashed line) at temperature $T = 298$ K (full line).

The SSRDF of the inner layer at half hydration are not presented, since the finite volume corrections cannot be calculated with enough accuracy when the density drops too rapidly (see the inset of Fig. 7).

V. SUMMARY AND CONCLUSIONS

We have presented the results of a layer analysis of the pair correlation functions of confined water obtained by computer simulation. Water is strongly adsorbed, due to the hydrophilic interaction with the substrate. Its density profile, which is almost independent of the temperature, shows the presence of a double layer of approximately 5 Å close to the substrate that we call the outer layer. At full hydration water fills the pore and we can calculate the structure of the set of molecules in the inner layer by excluding the molecules in the outer layer. The SSRDF of the molecules in the inner layer are very similar to those of bulk water. In particular the structure of the confined water in the inner layer at $T = 270$ K almost coincides with the structure of bulk water at ambient temperature, thus explaining why confined water can be supercooled down to lower temperatures than bulk water.

On the contrary the microscopic structure of water belonging to the outer layer differs from that of bulk water. In particular the oxygen–oxygen pair correlation function does not show any signature of the tetrahedral arrangement characteristic of bulk water. This is in agreement with experimental findings[8] and supported by previous computer simulation analysis of the distortion of the hydrogen bond network of confined water.[17] Moreover the SSRDF calculated for the outer layer are almost insensitive to temperature and hydration level. The first observation explains why the temperature derivatives of the RDF look so similar to those of bulk water.[9] The second suggests that the structure of water in the inner layer can be safely studied in a real diffraction experiment, looking at the difference between the data collected at different hydration levels. We stress finally that the analysis of the dynamical behavior of the molecules confined in the outer layer suggests that they are in a glassy state already at ambient temperature.[28] As a consequence their relative orientations must be strongly distorted relative to the bulk, in agreement with what found in the present analysis. The absence of tetrahedral order in the outer layer is also responsible for the lower nucleation temperature upon lowering the hydration level.

[1] A review, although not exhaustive, of thermodynamics, structural and dynamical properties can be found in M. A. Ricci, and M. Rovere, J. Phys. IV **10**, 187 (2000); M. A. Ricci, F. Bruni, P. Gallo, M. Rovere, and A. K. Soper, J. Phys.: Condens. Matter **12**, A345 (2000).

[2] T. M. Truskett, P. G. Debenedetti, and S. Torquato, J. Chem. Phys. **114**, 2401 (2001).

[3] V. P. Denisov and B. Halle, Faraday Discuss. **103**, 227 (1996).

[4] M. C. Bellissent-Funel, K. F. Bradley, S. H. Chen, J. Lal, and J. Teixeira, Physica A **201**, 277 (1993).

[5] M. J. Benham, J. C. Cook, J. C. Li, D. K. Ross, P. L. Hall, and B. Sarkissian, Phys. Rev. B **39**, 633 (1989).

[6] M. C. Bellissent-Funel, R. Sridi-Dorbez, and L. Bosio, J. Chem. Phys. **104**, 10023 (1996).

[7] F. Bruni, M. A. Ricci, and A. K. Soper, J. Chem. Phys. **109**, 1478 (1998).

[8] A. K. Soper, F. Bruni, and M. A. Ricci, J. Chem. Phys. **109**, 1486 (1998).

[9] D. C. Steytler and J. C. Dore, Mol. Phys. **56**, 1001 (1985).

[10] M. C. Bellissent-Funel, S. H. Chen, and J. M. Zanotti, Phys. Rev. **51**, 4558 (1995).

[11] S. H. Chen, P. Gallo, and M. C. Bellissent-Funel, Can. J. Phys. **73**, 703 (1995).

[12] S. H. Lee, J. A. McCammon, and P. J. Rossky, J. Chem. Phys. **80**, 4448 (1984); S. H. Lee and P. J. Rossky, *ibid.* **100**, 3334 (1994).

[13] E. Spohr, J. Chem. Phys. **106**, 388 (1997).

[14] J. X. Fang, W. H. Marlow, J. X. Lu, and R. R. Lucchese, J. Chem. Phys. **107**, 5212 (1997).

[15] S. B. Zhu and G. W. Robinson, J. Chem. Phys. **94**, 1403 (1991).

[16] E. Spohr, C. Hartnig, P. Gallo, and M. Rovere, J. Mol. Liq. **80**, 165 (1999).

[17] C. Hartnig, W. Witschel, E. Spohr, P. Gallo, M. A. Ricci, and M. Rovere, J. Mol. Liq. **85**, 127 (2000).

[18] J. M. Zanotti, M. C. Bellissent-Funel, and S. H. Chen, Phys. Rev. E **59**, 3084 (1998).

[19] M. C. Bellissent-Funel, S. Longeville, J. M. Zanotti, and S. H. Chen, Phys. Rev. Lett. **85**, 3644 (2000).

[20] F. Venturini, P. Gallo, M. A. Ricci, A. R. Bizzarri, and S. Cannistraro, J. Chem. Phys. **114**, 10010 (2001).

[21] General information on Vycor glass is available from Corning Glass Works OEM Sales Service, Box 5000, Corning, NY 14830.

[22] M. Rovere, M. A. Ricci, D. Vellati, and F. Bruni, J. Chem. Phys. **108**, 9859 (1998).

[23] H. J. C. Berendsen, J. R. Grigera, and T. P. Straatsma, J. Phys. Chem. **91**, 6269 (1987).

[24] A. K. Soper, J. Phys.: Condens. Matter **9**, 2399 (1997).

[25] B. M. Ladanyi and M. S. Skaf, Annu. Rev. Phys. Chem. **44**, 335 (1993).

[26] M. P. Allen and D. J. Tildesley, *Computer Simulation of Liquids* (Oxford University Press, Oxford, 1987).

[27] O. Glatter and O. Kratky, *Small Angle X-ray Scattering* (Academic, New York, 1992).

[28] P. Gallo, M. Rovere, and E. Spohr, Phys. Rev. Lett. **85**, 4317 (2000); J. Chem. Phys. **113**, 11324 (2000).